Available online at www.sciencedirect.com

SciVerse ScienceDirect

Energy Procedia 00 (2013) 000–000

Energy Procedia

www.elsevier.com/locate/procedia

SolarPACES 2013

# Wind Load Reduction for Light-Weight Heliostats

A. Pfahl[a]*, A. Brucks[b], C. Holze[b]

[a]*German Aerospace Centre (DLR), Institute of Solar Research, Pfaffenwaldring 38-40, 70569 Stuttgart, Germany*
[b]*toughTrough GmbH, Fahrenheitstrasse 1, 28359 Bremen, Germany*

**Abstract**

At SolarPACES 2012 conference a new heliostat concept was presented. It is equipped with wireless communication, sandwich facets, wind protection devices for wind load reduction, rim drives with winch wheels and ground anchor foundation. Crucial for the development of the light-weight structures is the precise determination of the maximum loads. By full scale wind load measurements the duration of the peak loads could be determined. They are caused by gusts with such short duration that their energy can be dissipated by shock absorbers protecting the structure. Furthermore, the wind loads can be reduced by wind protection devices. For the design-relevant stow position, a reduction in structural loading of 40 % can be achieved by the wind protection devices as wind tunnel tests have shown. The reduced loading has a significant impact on the dimensioning and cost of the structure and foundation of the heliostat. The systems for wind load reduction can be used for any kind of heliostat to reduce weight and cost.


Selection and peer review by the scientific conference committee of SolarPACES 2013 under responsibility of PSE AG.

*keywords*: heliostat, wind loading, wind protection devices, shock absorber

**Nomenclature**

| | |
|---|---|
| $\alpha$ | elevation angle [°] |
| $\beta$ | angle of wind relative to heliostat faces [°] |
| $c_{MHy}$ | $= M / (A\ h\ 1/2\ \rho\ V^2)$ dimensionless hinge moment coefficient [-] |

* Corresponding author. Tel.: +49-711-6862-479; fax: +49-711-6862-8032.
*E-mail address:* Andreas.Pfahl@dlr.de

1876-6102 © 2013 The Authors. Published by Elsevier Ltd.
Selection and peer review by the scientific conference committee of SolarPACES 2013 under responsibility of PSE AG.
doi: 10.1016/j.egypro.2014.03.021

| | |
|---|---|
| $c_p$ | $= (p - p\infty)/(1/2\ \rho V^2)$ dimensionless pressure coefficient [-] |
| $A$ | mirror area [m²] |
| $h$ | height of mirror panel [m] |
| $H$ | height of elevation axis [m] |
| $M_{Hy}$ | hinge moment [Nm] |
| $p, p\infty$ | local pressure [Pa], undisturbed pressure [Pa] |
| $r_a$ | aspect ratio [-] |
| $\rho$ | density of air [kg/m³] |
| $V$ | velocity [m/s] |

## 1. Introduction

### *1.1. Heliostat-Concept*

Several approaches for cost reduction of heliostats, which fit well to each other, are combined to a new heliostat concept (Fig. 1., [1]) to achieve the current challenging cost objectives: The wind loads are reduced by appropriate manipulators which reduce weight and cost of the heliostat structure and the ground anchor foundation. Laminated mirror facets are of high reflectivity and shape accuracy and of low weight. The low weight is advantageous for the dimensioning of the bearings and regarding energy consumption. Energy consumption is further reduced by a highly efficient drive train. Thus, small capacity of the wireless energy supply of the autonomous heliostat is sufficient which reduces significantly its cost.

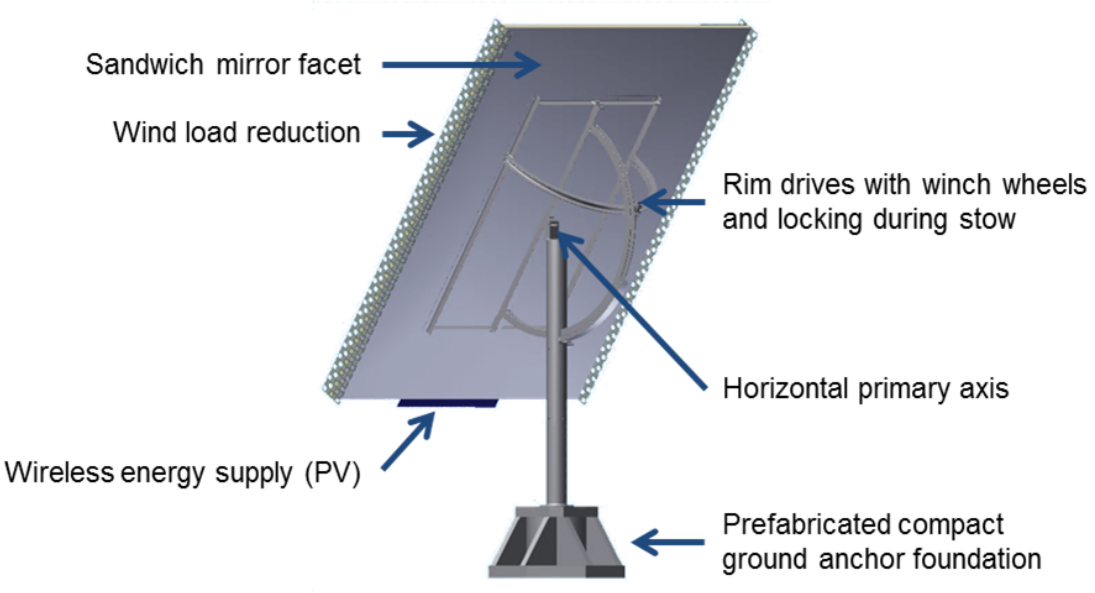


Fig. 1. Autonomous light-weight heliostat with rim drives

### *1.2. Determination of peak wind loads*

The main loading of heliostats is caused by wind. Wind events can be classified into micrometeorological and macrometeorological wind events [2]. Macrometeorological wind events are mainly caused by changes in weather and season and change in a scale down to one hour. Micrometeorological wind events are caused mainly by obstacles on the ground that disturb the wind and change in a scale up to 10min. To determine the impact of the

fluctuations caused by micrometeorological wind events in interaction with the investigated structure the loads must be measured in a time interval of minimum 10 min (at real scale) to capture all possible micrometeorological wind events. In the corresponding wind tunnel experiments the micrometeorological fluctuations must be modeled according to the length scale [2].

The higher the resolution of the wind load measurements the higher are the measured peak values because peaks of small duration will be detected with higher probability. To determine the required resolution it is commonly assumed that only gusts larger than the structure are relevant because smaller gusts don't encompass the whole structure and are therefore only of local impact and cannot lead to the peak loading of the complete structure in the design relevant stow position. Often a value of 2-3 seconds is used [3, p. 5]. However, this value might be appropriate for large buildings but not for small heliostats. For the investigated heliostat for example with maximum extension of 4m and for wind speeds of 5.5 m/s the duration of gusts that encompass the complete heliostat is only 0.7 seconds. Therefore, in this study high resolution pressure measurements were realized.

### *1.3. Relevant gust size and load case*

It can be assumed that the fluctuations of the wind velocity are a superposition of eddies with different sizes and, hence, frequencies [4]. An eddy may be represented as a mass of fluid rotating around a center [2, pp. 20ff]. To reach peak loads, eddies in the size of width and height of the heliostat are decisive. Eddies which are smaller than the mirror panel have only local impact. Eddies larger than the panel size have their high speed core regions above the heliostat. The rotational speed, and therefore the energy that can be transmitted, reduces strongly with the distance to the eddy's core [2, pp. 20ff]. Furthermore, the vertical velocity component at panel height of larger eddies is lower which leads to lower hinge moments for horizontal panel. Therefore, eddies with their center in the height of the heliostats are causing the peak loads. The size of these eddies are in the range of the chord length of the mirror panel which is about double the heliostat's height. Eddies considerably larger than cord length are only indirectly of impact because they may transport eddies of relevant size and increase their velocity. Hence, the mean velocity of the relevant gusts may be above the mean level of the complete flow.

The dimensionless pressure coefficients $c_p$ are lowest when the heliostat is in stow position (horizontal mirror plane). Nevertheless, most of the wind load components reach their highest values for stow conditions because of the high storm wind speed compared to operational wind speed. Therefore, the stow position is studied in detail. Only for the azimuth drive the wind loading during operation (moment about vertical axis) is decisive.

Wind loads can be reduced by wind fences for high field densities [5],[6]. The field density decreases with distance from the tower because usually the heliostats are positioned in a staggered configuration with a row distance increasing with distance to the tower to avoid optical blocking. For low field densities the benefits regarding peak loads wear off from the third row on. Therefore, the maximum loads in a heliostat field are similar to the ones of an isolated heliostat, even if a wind fence is installed. Hence, the isolated heliostat without fence in stow position is the most relevant load case and is investigated in this study.

## 2. Full scale wind load measurements: duration of peak loads

### *2.1. Description of test set up*

The in-field measurements were performed on an isolated full-scale heliostat set up (Fig. 2) in an area which complies with area category II [7]. The heliostat and its test equipment were set up in Lower Saxony, municipality Lilienthal, at a countryside area almost without any houses, trees and bushes, or other objects that could disturb the wind (Lat 53°9'59.66 N, Long 8°50'0.40 E). For the performed full-scale tests the single, isolated 8 m² (2.5m x 3.2m) heliostat was equipped with 84 differential pressure gauges (compare Fig. 2, right) to collect direct information of the local pressure distribution. Strain gauges for the measurement of the hinge moment were not foreseen because measureable deformation of the pylon occurs only for rare high wind speeds.

The chosen coordinate system for azimuth and elevation follows Peterka [8]. The orientation of the coordinate system with respect to the heliostat and the geographic orientation are shown in Fig. 2, left. The heliostat facet (mirror surface) was facing the prevailing westerly winds with compass reading 308°. This angle was fixed during

measurements. Two angles define the measured configuration: the elevation $\alpha$ and the wind direction $\beta$. The wind direction $\beta$ is defined relative to the heliostat facet with 0° of wind square on the facet.

Measurements were taken for elevation angles 0°, 5°, 30°, 45°, 60° and 90°. Pressure, wind velocity and wind direction readings were stored on hard disk. Results are presented for the design case as deducted in section 1.


Fig. 2: left: Heliostat (size 8m²) in the field, municipality Lilienthal, Germany. The chosen coordinate system according to Peterka is drawn on the facet. In the background: telescopic mast with sensors. Right: The heliostat is equipped with 84 differential pressure ports. (1) facet, (2) supporting structure, (3) elevation inclination, (4) pylon, (5) pedestal, (6) pressure tubing and instrumentation boxes, (7) pressure ports.

### *2.2. Results*

With the pressure distribution the time depended behavior of the hinge moment coefficient $c_{MHy}$ (moment about horizontal primary axis, definition according to [3]) was calculated. Overall dimensionless coefficients were calculated as weighted summation of the point pressures following the method described by [9]. Fig. 3 shows the 10s time interval at which the maximum peak value of a 10 min measurement occurred (at about 7 s). It seems that an eddy of about 0.7 s duration (between 6.5 s and 7.2 s) caused the peak. The mean wind velocity at this time interval was 5.5 m/s. Hence, the duration of the eddy is in accordance with the expected value (compare paragraph 1.2).

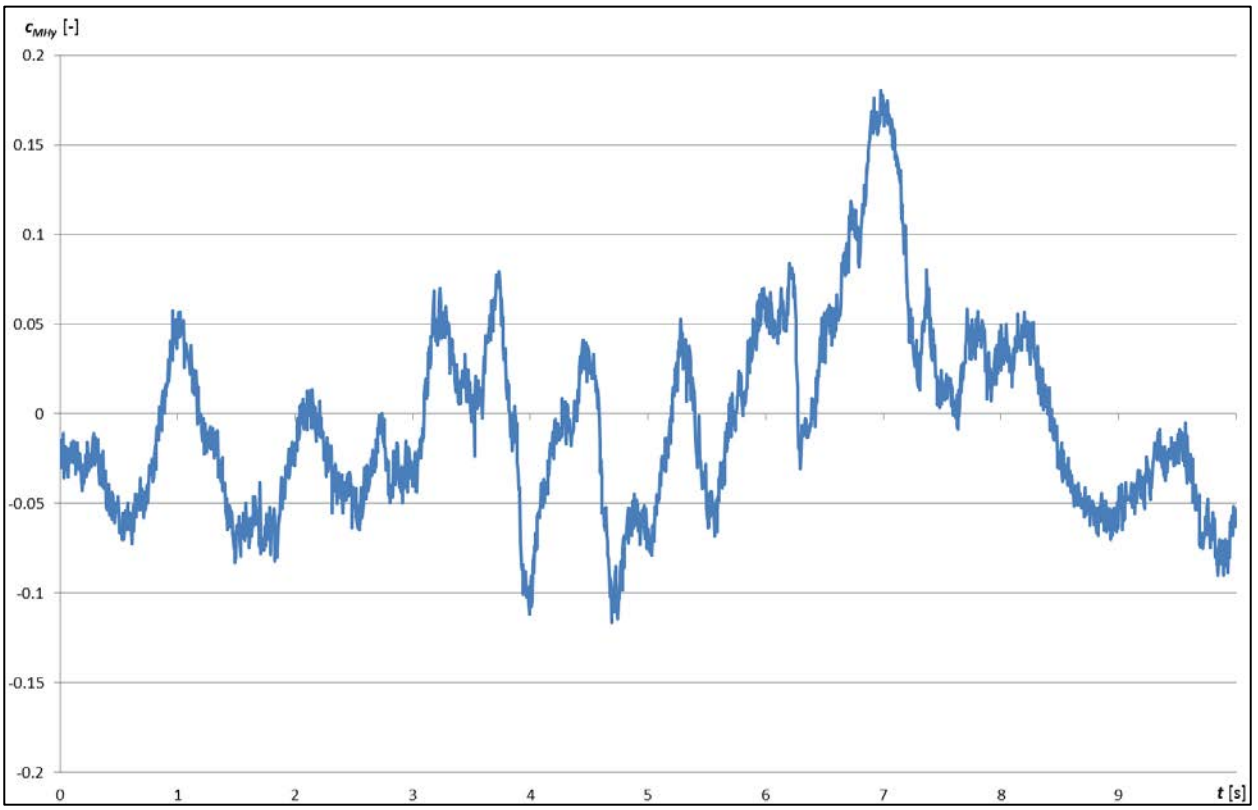


Fig. 3. Hinge moment coefficient over time, elevation 0° (stow position).

## 3. Boundary layer wind tunnel measurements: load reduction by wind protection devices

### *3.1. Description of test set up*

To simulate boundary layer conditions of atmospheric flows typical at solar power plant sites, a sophisticated simulation technique has been developed using a specific set-up of the blocks and baffles on the wind tunnel floor. At the boundary layer wind tunnel of the University of the Armed Forces, Munich, both velocity and turbulence distributions have been realized. Fig. 4, right, shows part of the equipment used and installation for the boundary layer simulation.

All measured operation conditions were defined by the orientation of the heliostat towards the incident wind vector: elevation angle $\alpha$ and wind direction angle $\beta$. For the tests, the isolated heliostat in scale 1:10 was mounted on the rotary plate wind tunnel floor, so that all angle variations of wind direction angle $\beta$ were adjusted automatically (Fig. 4, left). The heliostat itself was also automated, so the elevation angle $\alpha$ is driven automatically as well.

Fig. 4. Left: Heliostat model with wind protection devices for wind load reduction mounted on rotary plate. Right: View of boundary layer simulation installation (partly, total length 12m) and heliostat model in the test section of the boundary layer wind tunnel of the University of Armed Forces (UniBW), Munich with a cross section of 1.9m by 1.9m.

### *3.2. Results*

Two configurations were compared: (i) clean configuration and (ii) reduced wind load where the heliostat edges were equipped with wind protection devices described by [1]. Overall dimensionless coefficients were calculated as weighted summation of the point pressures following the method described by [9].

The reduction in $c_{MHy}$ is significant due to the manipulation of the pressures at the edges. Depending on the configuration of wind protection devices reduction in structural loading of 40% is achieved for stow position with horizontal mirror panel.

## 4. Wind load assumptions for first prototype

### *4.1. Wind load on structure*

For the layout of the first prototype a maximum storm wind speed of 42 m/s at 10 m height is assumed which is a typical value. Peak values are caused by gusts in the size of the heliostat (compare paragraph 2.2). The maximum extension of the 16m² prototype (panel size 3.2m x 5m) will be 6 m. Assuming a wind profile according to the power law with an exponent of 0.15 the maximum wind velocity at panel height in stow position ($H$=3.1 m) is 35 m/s. Hence, the duration of relevant gusts is 0.17s. For about half the time (0.9s) the resulting moment is above half the peak value. Because of the short duration of the peak loads it is possible to reduce them by shock absorbers.

According to [6] the peak hinge moment coefficient for the given aspect ratio of $r_a$=0.64 is $c_{m,\,peak}$ =0.2. Due to wind protection devices the hinge moment reduces by 40% (compare 3.2) as typical value. The resulting peak hinge moment is $M_{Hy}$=3kNm. For primary tests it is defined that the shock absorber should react if the hinge moment increases by half of its maximum value which means that they don't react at operational wind conditions. The graph in Fig. 5, dashed line, shows the defined load case representing a shock at storm conditions. This load case is used to dimension the shock absorbers.

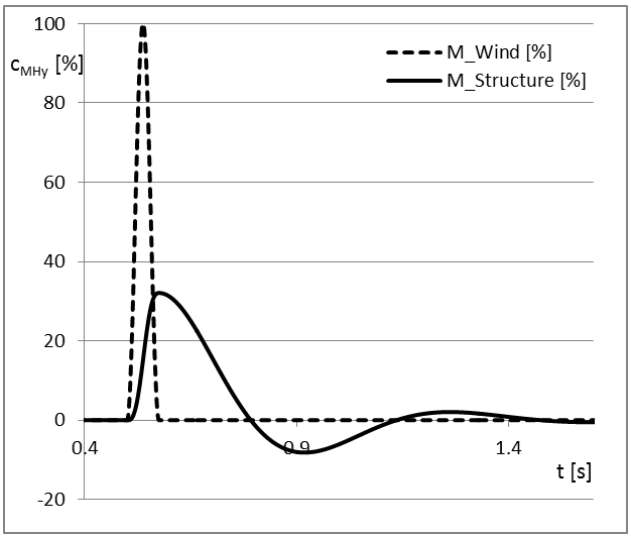


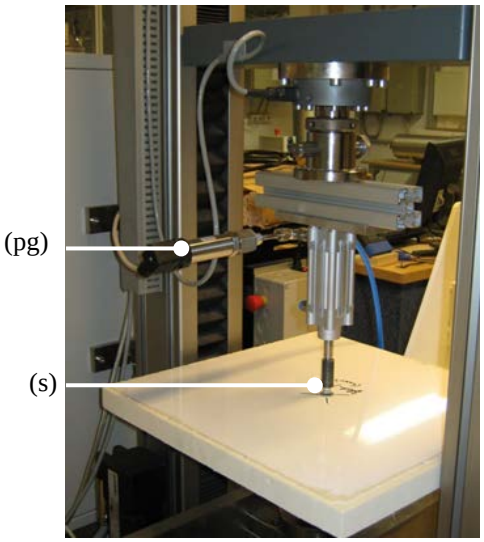


Fig. 5. (Left) Definition of load case representing a shock caused by a storm gust (dashed line) to dimension shock absorber. The figure shows dynamic behaviour of the reference system with wind induced torque moment and structural reaction moment (solid line). (Right) Testing the interaction between sandwich panel and shock absorber at low and high frequencies. (s) shock absorber, (pg) pressure gauge.

### *4.2. Peak load reduction by shock-absorber system*

For the design of the first heliostat prototype with a facet size of 16m$^2$ the moment loading caused by wind has been analyzed for typical operation and stow positions. The structural deformation of the reflector and supporting structure were minimized preventing any plastic deformation of the structural components as well as the drives. To reduce the loads high structural short time shocks/forces to the heliostat facet caused by gusts are limited. Typical active and passive actuators to be integrated into the drive chain, mainly to act as interface between the heliostat facet and the rim wheels, have been analyzed and tested (Fig. 5, right). With respect to the design layout of the prototype as well as the expected frequencies/shock duration a passive damping system has been selected to minimize transferred shocks to the rim wheels.

The actuator system absorbs nearly all frequencies higher than 10Hz respectively transferred forces/moments. Practical tests showed good agreement between predicted and measured behavior. The integration of shock absorber elements can decrease the relevant peak moment loadings – related to gusts with frequencies > 10 Hz – to the rim wheels and therefore also the drive/locking unit. Theoretical and experimental tests showed potential of more than 30% of the dynamic forces and moments respectively (Fig. 5 left, solid line).

## 5. Conclusions

By wind protection devices the design relevant hinge moment of heliostats in stow position can be reduced by 40%. Furthermore, the peak loads can be reduced by another 30% through shock absorbers. This is possible because the peak loads are of relatively short duration as was found by full scale measurements. Hence, the cost of facets, bearings, locking devices, pylon and foundation can be drastically reduced by wind protecting systems. They will be tested soon at a 16m² prototype.

## Acknowledgements

The German Federal Ministry for the Environment, Nature Conservation and Nuclear Safety (BMU) financed partly the wind tunnel investigations by the project HydroHelio$^{TM}$ (code 0325123B).

## References


[1] Pfahl, A., Randt, M., Kubisch, S., Holze, C., Brüggen, H., Autonomous Light-Weight Heliostat with Rim Drives, Solar Energy 2013, 92, pp 230–240.

[2] Cook, N.J., The designer's guide to wind loading of building structures – Part 1: Background, damage survey, wind data and structural classification. Butterworths, London 1985.

[3] Peterka, J.A., Derickson, R.G., Wind load design methods for ground based heliostats and parabolic dish collectors, Report SAND92-7009, Sandia National Laboratories, Springfield, 1992.

[4] Geurts, C.P.W., Wind-Induced Pressure Fluctuations on Building Facades, Dissertation, Eindhoven, 1997.

[5] Peterka, J.A., Hosoya, N., Bienkiewicz, B., Cermak, J.E., Wind Load Reduction for Heliostats. Report SERI/STR-253-2859, Solar Energy Research Institute, Golden, Colorado, USA, 1986.

[6] Pfahl, A., Buselmeier, M., Zaschke, M., Determination of Wind Loads on Heliostats, Proc. SolarPACES 2011 conference, Granada, Spain.

[7] Eurocode 1: Actions on structures – general actions - part 1-4: Wind actions ,Technical Committee CEN/TC250 Structural Eurocodes.

[8] Peterka, J. A., Tan, Z., Bienkiewicz, B., Cermak,J. E., Wind loads on heliostats and parabolic dish collectors,SERI/STR-253-3431, 1988.

[9] Hosoya, N., Peterka, J. A., Gee, R. C., Kearney, D. (2008): Wind Tunnel Tests of Parabolic Trough Solar Collectors, NREL/SR-550-32282.